International Geology Review, Vol. 44, 2002, p. 383–401.

Steady-State Failure Equilibrium and Deformation of Intraplate Lithosphere

MARK D. ZOBACK, JOHN TOWNEND, AND BALZ GROLLIMUND

Department of Geophysics, Stanford University, Stanford, CA 94305-2215

Abstract

We present a simple conceptual model in which the entire lithosphere is in steady-state failure equilibrium—brittle failure in the upper crust and ductile creep in the lower crust and upper mantle—in response to finite, buoyancy-related plate tectonic forces. We demonstrate that, in the context of finite plate driving forces, high crustal strength provides a first-order constraint on the rate at which intraplate lithosphere deforms. For strike-slip stress states and moderate intraplate heat flow (~60 ± 6 mW m^{-2}), average strain rates are less than 10^{-17} s^{-1}, consistent with the upper bounds imposed by rigid-plate assumptions inherent in plate tectonic reconstructions as well as with average intraplate strain rates measured by very long baseline interferometry (VLBI). Because regions of higher heat flow are characterized by low effective viscosity in the lower crust and upper mantle, the available plate driving forces are sufficient to cause faster creep at depth (and higher seismicity rates in the overlying brittle crust) than in in regions of lower heat flow. We suggest that the current debate over whether intraplate deformation is best viewed in terms of a deforming continuum or as rigid crustal blocks separated by relatively narrow and weak fault zones may be a false dichotomy. We illustrate this for the Coast Ranges and Central Valley of western California. In the Coast Ranges, a region of high heat flow, high deformation rates are expected because of correspondingly high temperatures in the lower crust and upper mantle. The adjacent Central Valley is characterized by very low heat flow and deforms at such a slow rate that it appears to behave as a rigid block. Finally, in the context of steady-state lithospheric failure equilibrium, we demonstrate that the Holocene concentration of intraplate seismicity in the New Madrid seismic zone can be explained in terms of the stress perturbation caused by retreat of the Laurentide ice sheet and anomalous upper mantle structure beneath the Late Precambrian Reelfoot rift.

Introduction

WE CONSIDER INTRAPLATE DEFORMATION in terms of a relatively simple steady-state "failure equilibrium" model of the lithosphere based on: (1) the finite magnitude of buoyancy-related plate tectonic driving forces, (2) the high frictional strength of the upper crust, and (3) the strong dependence on temperature of the rheology of the ductile lower crust and upper mantle.

First, we discuss the origin of the high frictional strength of the upper crust and the mechanism by which an efficient intraplate stress guide transmits plate driving forces over thousands of kilometers. Second, we discuss the way in which the finiteness of plate driving forces limits intraplate strain rates. When the lower crust and upper mantle are relatively cold (such as in shield areas), deformation occurs so slowly that intraplate lithosphere appears to be rigid. In areas of higher lithospheric temperatures, appreciable intraplate deformation can occur. Third, we discuss the manner in which the observed localization of intraplate deformation might be related to variations in lithospheric rheology. Specifically, high rates of localized deformation are expected to exist in areas of relatively low effective viscosity (due to either high temperature or anomalous composition), and to be manifest as relatively high rates of intraplate seismicity.

It has been generally concluded that the forces responsible for plate motions (and intraplate stress fields) are fundamentally associated with gradients in the density and thickness of the lithosphere (e.g., Forsyth and Uyeda, 1975; Jones et al., 1996; Flesch et al., 2000, 2001). From considerations of tectonic driving forces (slab pull and ridge push), thrust-zone topography, and elastic plate deformation, several authors have estimated the total force available to cause relative plate motions at 1–5 × 10^{12} N m^{-1} (Forsyth and Uyeda, 1975; Turcotte and Schubert, 1982; Bott and Kusznir, 1984; Kusznir,

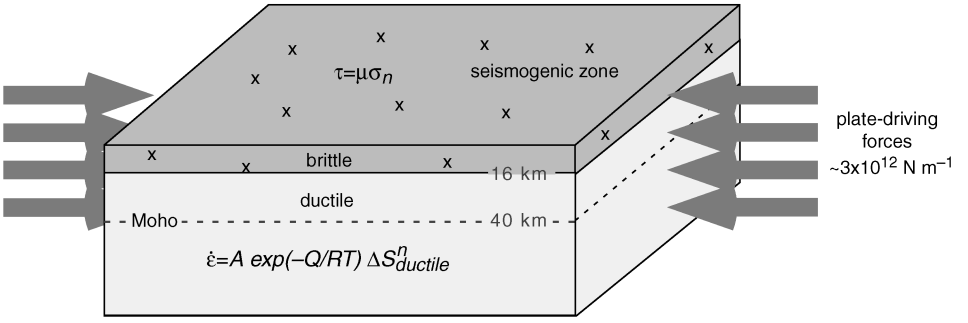

FIG. 1. A schematic illustration of steady-state failure equilibrium in the lithosphere. The lithosphere carries finite plate driving forces of approximately known magnitude (~3 × 10^{12} N m^{-1}). Because the lower crust and upper mantle deform in response to any finite plate driving force, the upper crust is progressively loaded to brittle failure, even in relatively stable intraplate areas that deform so slowly as to appear rigid (from Zoback and Townend, 2001).

1991). In the sections that follow, we will use an average value of 3 × 10^{12} N m^{-1} as a mid-range estimate.

Our conceptual model of the lithosphere, illustrated in Figure 1, incorporates a number of simple working principles. We consider the lithosphere to comprise the crust and the portion of the upper mantle that carries buoyancy-related tectonic forces. As is well known, the lithosphere is rheologically as well as compositionally stratified. The uppermost 15–20 km of the lithosphere (the upper crust) deforms through predominantly brittle frictional failure that is revealed most obviously by earthquakes. Numerous authors have noted that combining Mohr-Coulomb frictional-failure theory (e.g., Jaeger and Cook, 1979) with laboratory-derived coefficients of friction (e.g., Byerlee, 1978) leads to the conclusion that the brittle strength of the crust is of the order of several hundred megapascals under hydrostatic pore pressure conditions, and vanishingly small as pore pressures approach lithostatic values (e.g., Hubbert and Rubey, 1959; Sibson, 1974).

At mid-crustal depths, temperatures are inferred to be sufficiently high that ductile failure mechanisms operate at lower differential stress levels than required for brittle faulting (Chen and Molnar, 1983; Sibson, 1983; Kohlstedt et al., 1995). Following previous authors, we represent the rheology of the ductile lower crust and lithospheric mantle using a power-law creep relationship (e.g., Brace and Kohlstedt, 1980). In this case, the ductile strain rate $\dot{\varepsilon}$ is given in terms of the differential stress $\Delta S_{ductile}$ by

$$\dot{\varepsilon} = A \exp\left(-\frac{Q}{RT}\right) \Delta S^{n}_{ductile}, \qquad (1)$$

where A, n, and Q are material parameters (the flow parameter, stress exponent, and activation energy, respectively), R is the gas constant, and T is the absolute temperature (Ranalli and Murphy, 1987). We presume that rock will deform at any depth in the crust and upper mantle by whichever mechanism (frictional faulting or power-law creep) requires the lower differential stress (Brace and Kohlstedt, 1980). It is likely that semi-brittle deformation occurs at mid-crustal depths; however, as will be seen below, we are interested in the overall size of the strength envelope as a function of depth, rather than its exact shape.

Another important feature of our conceptual model is that the lithosphere is in a state of failure equilibrium. This is to some degree intuitive as far as the lower crust and upper mantle are concerned, because $\dot{\varepsilon}$ is finite for any non-zero differential stress (Eq. 1). Thus, any force applied to the lithosphere causes the lower crust and upper mantle to undergo ductile creep. If we assume in addition that the ductile portions of the lithosphere are mechanically coupled to the brittle crust, then ongoing ductile creep progressively loads the upper crust to the point of failure.

Three independent lines of evidence suggest that a state of failure equilibrium exists within intraplate continental upper crust: (1) seismicity induced by small increases in fluid pressure associated with

fluid injection (e.g., Healy et al., 1968; Pine et al., 1983; Zoback and Harjes, 1997) or reservoir impoundment (e.g., Simpson et al., 1988; Roeloffs, 1996); (2) earthquake triggering by other earthquakes (e.g., Stein et al., 1992, 1997); and (iii) *in situ* stress measurements in deep boreholes, which are consistently found to approximately equal those predicted using Mohr-Coulomb frictional failure theory (see summary by Townend and Zoback, 2000) for laboratory-derived coefficients of friction of 0.6–1.0 (Byerlee, 1978). In the context of our model, upper-crustal stress is expected to be high in both relatively stable Phanerozoic intraplate regions and in Archean and Proterozoic shield areas, as observed with the deep borehole stress measurements made in southeastern Germany (Brudy et al., 1997) and Sweden (Lund and Zoback, 1999). This is discussed at greater length below.

Another important component of the failure equilibrium model of lithospheric deformation is that the total force available to cause intraplate strain is limited to that provided by tectonic processes. The cumulative strength of the lithosphere is the sum of the brittle strength of the upper crust and the ductile strength of the lower crust and upper mantle. Thus, by invoking the constraint that there is a finite force available to cause deformation (e.g., $\sim 3 \times 10^{12}$ N m^{-1}) and assuming that the upper crust, lower crust, and lithospheric mantle are fully coupled, an average strain rate for the whole lithosphere can be estimated (Liu and Zoback, 1997). As will be argued below, a large fraction of the total plate driving force is consumed by deforming the upper crust through faulting (and noting that the brittle strength of the crust is independent of composition), and the remaining force is available to cause ductile deformation of the lower crust and upper mantle. Hence, stress levels in the upper crust are controlled by its frictional strength, and lithospheric strain rates are controlled by the remaining force and the rheological parameters of the ductile lithosphere. As discussed by Zoback and Townend (2001), maximum intraplate lithospheric strain rates can be estimated using the constraint that the cumulative strength of the lithosphere, S_L, given by

$$S_L = \int_0^D \Delta S dz \qquad (2)$$

(England and Houseman, 1986), is equal to the available plate driving force, where D is the thickness of the lithosphere and ΔS is the differential stress at which deformation occurs, which varies as a function of depth. In the sections below, we investigate the roles played by upper-crustal critical stress states and hydrostatic pore pressures in controlling the vertical distribution of strength in intraplate lithosphere and the rates at which intraplate lithosphere deforms.

The Crustal Stress Guide

As mentioned above, *in situ* stress magnitude data collected at depths of up to 9.1 km at a number of locations worldwide indicate without exception that differential stresses increase with depth at gradients consistent with frictional faulting theory and laboratory-measured coefficients of friction of 0.6–1.0. This is clearly illustrated by the profile of deep stress measurements in the Kontinentales Tiefbohrprogramm der Bundesrepublik Deutschland (KTB) borehole shown in Figure 2, where stress is observed to increase with depth at a rate compatible with Mohr-Coulomb faulting theory given a friction coefficient of 0.6–0.7 and the observed hydrostatic pore pressure (see also Brudy et al., 1997). Further evidence that the crust at the KTB site is in a state of frictional equilibrium is provided by the fact that microearthquakes were induced at ~9 km depth by extremely small increases in fluid pressure (Zoback and Harjes, 1997).

Figure 3 (after Townend and Zoback, 2000) is a compilation of *in situ* stress measurements from several deep boreholes worldwide (including the KTB borehole). The data correlate extremely well with predictions made using frictional faulting theory and laboratory-derived coefficients of friction; the dashed lines are theoretically expected relationships representing failure equilibrium for frictional coefficients ranging between 0.6 and 1.0, the same range as that observed in the laboratory (Byerlee, 1978). Additional data collected at shallower depths in the crust (<3 km) substantiate the observation that the upper crust is critically stressed according to Mohr-Coulomb frictional failure theory (see reviews by McGarr and Gay, 1978 and Zoback and Healy, 1992).

Because frictional strength depends on pore pressure, it is important to note that the high upper-crustal strength implied by Figures 2 and 3 is associated with essentially hydrostatic pore pressures. Townend and Zoback (2000) summarized the results of hydraulic tests conducted at length scales of 10–1000 m and depths as great as 9 km (as well

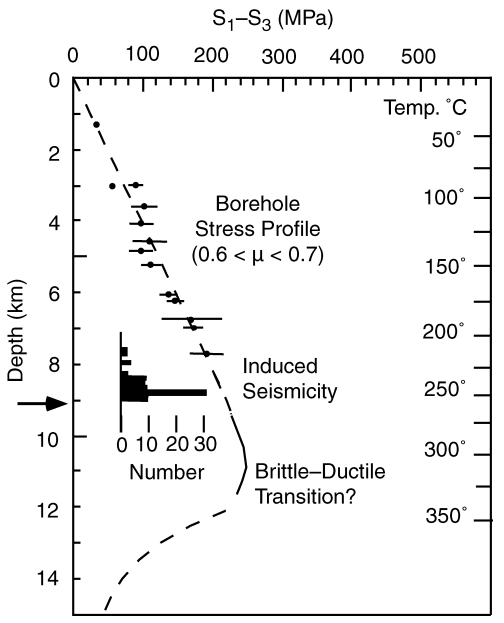

FIG. 2. Maximum differential stress as a function of depth in the KTB scientific research borehole (from Zoback and Harjes, 1997). Note that the strength measurements fall along a theoretical strength curve predicted using Mohr-Coulomb frictional failure theory and a coefficient of friction of 0.6–0.7, consistent with laboratory measurements. The depths at which microseismicity was triggered by small increases in fluid pressure are shown in histogram form. The orientation of maximum horizontal stress is relatively constant from 3 to 8 km (Brudy et al., 1997).

as the migration rates of induced seismicity over distances of up to several kilometers) and observed that upper-crustal permeability is of the order of 10^{-17} to 10^{-16} m^2, or three to four orders of magnitude higher than that of core samples studied in the laboratory at equivalent pressures. Geothermal and metamorphic data also indicate that the permeability of the upper crust exceeds 10^{-18} m^2 throughout the brittle regime (Manning and Ingebritsen, 1999).

The mechanism responsible for high crustal permeability is fundamentally related to the observation that the crust is in a state of frictional equilibrium. Using data from the Cajon Pass, Long Valley, and Yucca Mountain USW-G1 boreholes, Barton et al. (1995) demonstrated that optimally oriented planes are hydraulically conductive, whereas non-optimally oriented planes are nonconductive. This conclusion is supported by data collected subsequently from boreholes in Dixie Valley, Nevada (Hickman et al., 1997; Barton et al., 1998), and a similar result was obtained by Ito and Zoback (2000) for faults and fractures intersecting the KTB main borehole at great depth. Another way of saying this is that the active faults that limit crustal strength are also responsible for maintaining pore pressures at hydrostatic values. These results (Fig. 4) clearly indicate that critically stressed faults act as fluid conduits and control large-scale permeability (Townend and Zoback, 2000; Zoback and Townend, 2001). The inset in Figure 4 illustrates the combined datasets in terms of the ratio of shear stress to effective normal stress. It is apparent that the mean of this ratio is approximately 0.6 for the conductive fractures (consistent with Mohr-Coulomb frictional failure on well-oriented faults), and only ~0.3 for the nonconductive fractures (indicating that those fractures are not critically stressed).

Thus, the presence of critically stressed faults in the crust keeps the brittle crust permeable and upper-crustal pore pressures close to hydrostatic values. Under these conditions, intraplate faults are able to sustain high differential stresses before failure.

One manifestation of high crustal strength is the efficient transmission of tectonic stress over distances of thousands of kilometers in intraplate regions, via what is in effect an upper-crustal stress guide. This was first observed in the conterminous United States and North America (Fig. 5, after Zoback and Zoback, 1980, 1989, 1991) and later on a global basis (Zoback, 1992). East of the western Cordillera, the direction of maximum horizontal stress measured throughout North America is remarkably consistent with the orientation of the plate-driving forces associated with the ridge-push force (Zoback and Zoback, 1991). In the following section we investigate how high crustal strength influences the rate of intraplate lithospheric deformation.

Limits on Intraplate Deformation Rates

The manner in which the magnitude of plate driving forces is related to lithospheric deformation can be investigated using strength envelopes that incorporate appropriate rheologies to represent the ductile behavior of the lower crust and lithospheric mantle. Differential stresses required for brittle and ductile deformation are computed as functions of depth, and then combined by presuming that the deformation mechanism operative at any depth is

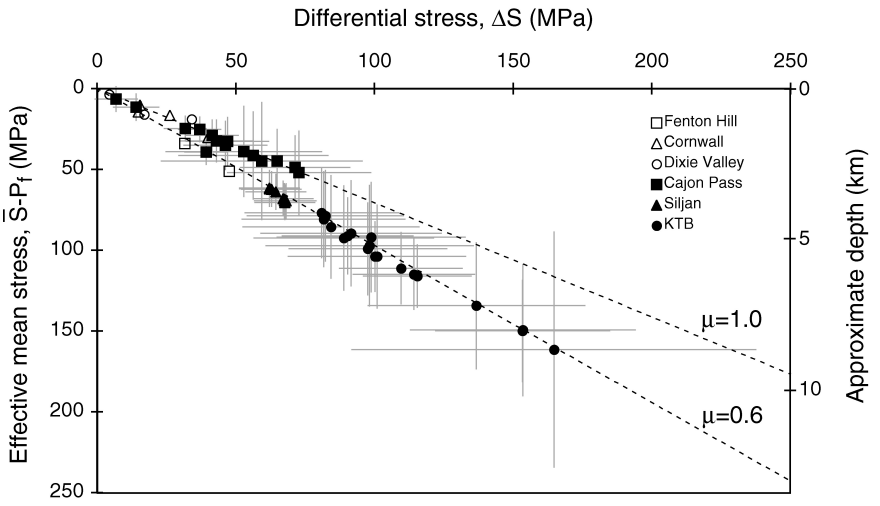

FIG. 3. Maximum differential stress measurements from six deep boreholes, illustrating that the upper crust is in a stress state consistent with that predicted using Mohr-Coulomb frictional failure theory and friction coefficients of 0.6 to 1.0 (modified from Townend and Zoback, 2000).

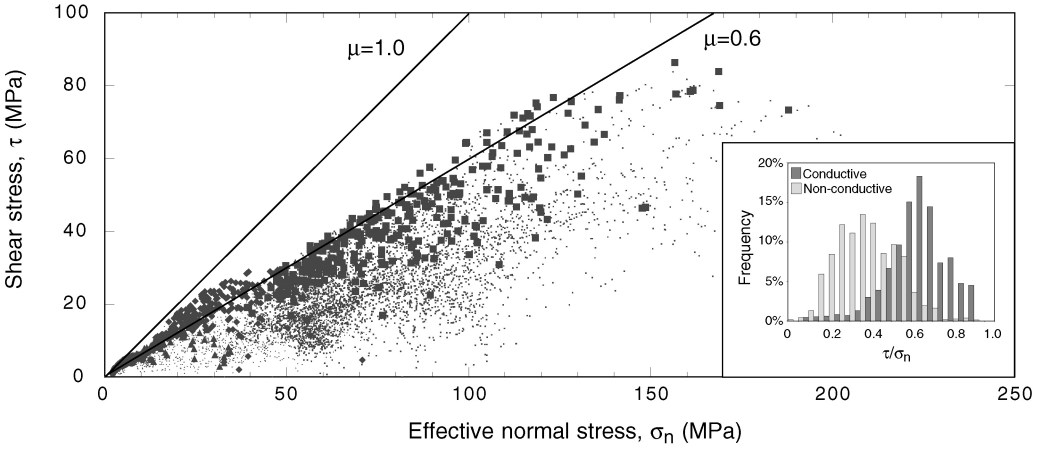

FIG. 4. Shear and effective normal stresses on fractures identified using borehole imaging techniques in the Cajon Pass, Long Valley, Nevada Test Site, and KTB boreholes (from Zoback and Townend, 2001; original data from Barton et al., 1995 and Ito and Zoback, 2000). The larger, filled symbols represent hydraulically conductive fractures and faults, and the dots represent non-conductive fractures. The inset figure illustrates the range in shear-to-normal stress ratio for the entire data set.

that which requires the lower stress. As illustrated in Figure 6, integrating this differential stress profile over the thickness of the lithosphere gives the cumulative force required to deform the lithosphere, here presumed to be ~3×10^{12} N m^{-1}. This approach is different from those used by several other authors (e.g., Sibson, 1983; Ranalli and Murphy, 1987; Kohlstedt et al., 1995) because the lithospheric strain rate is not an arbitrarily chosen model parameter. Although the sharp "nose" in the strength profiles at mid-crustal depths is rather non-physical in light of likely semi-brittle deformation processes, as

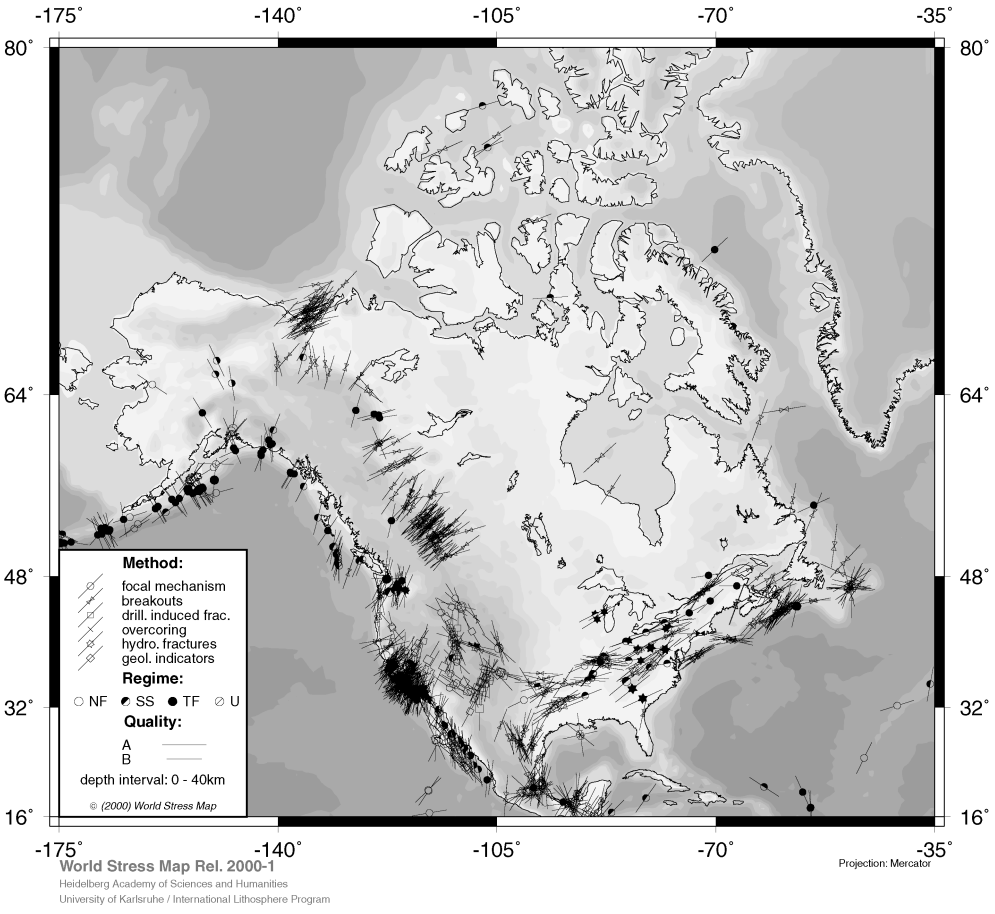

FIG. 5. Maximum horizontal stress directions in North America. These data are from the World Stress Map database, maintained by the Heidelberg Academy of Sciences, http://www-wsm.physik.uni-karlsruhe.de/index.html.

long as these processes do not dramatically alter crustal strength, the cumulative area under the curve will not be altered significantly.

For most intraplate areas, a test of such models is that the estimated intraplate lithospheric strain rate not exceed approximately 10^{-17} s^{-1}, in order to be consistent with plate tectonic reconstructions (Gordon, 1998). For example, throughout the ~100 Ma duration of the opening of the Atlantic Ocean, no more than ~100 km of shortening took place in the ~10,000 km-wide African or South American plates. Thus, the maximum intraplate strain rate is approximately 10^{-17} s^{-1}. Additionally, very long baseline interferometry (VLBI) measurements place an upper bound of 10^{-17} s^{-1} on strain rates within the North American plate (Gordon, 1998), and average seismic strain rates in the eastern United States are 10^{-19} to 10^{-18} s^{-1} (Anderson, 1986). We conclude from this that intraplate continental lithosphere does not deform more rapidly than ~10^{-17} s^{-1} in most areas over geological time scales.

As discussed by Zoback and Townend (2001), we consider a generalized lithospheric structure composed of a 16 km-thick felsic upper crust (with the rheological properties of dry Adirondack granulite), a 24 km-thick mafic lower crust (dry Pikwitonei granulite), and a 60 km-thick lithospheric mantle (wet Aheim dunite), based on the composite velocity-depth model obtained by Christensen and Mooney (1995), and rheological coefficients determined by Chopra and Paterson (1981), Carter and Tsenn (1987), and Wilks and Carter (1990).

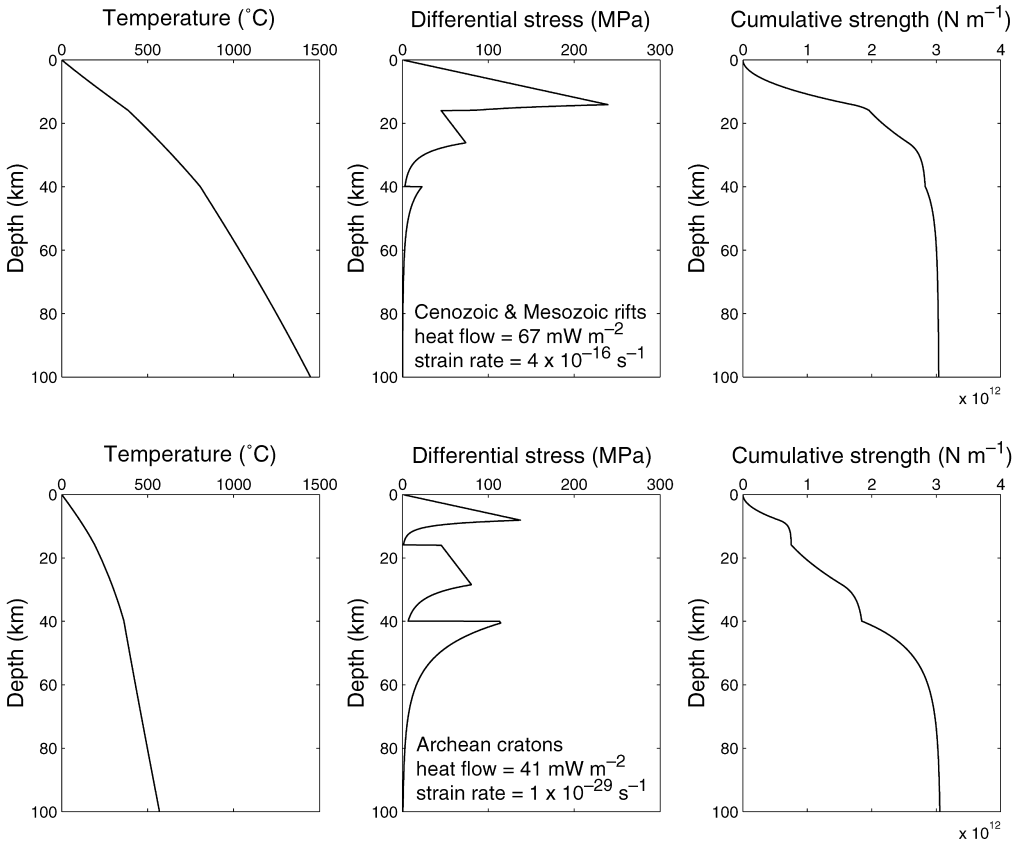

FIG. 6. A comparison between theoretical temperature, differential stress, and cumulative strength profiles for two representative intraplate regions, an area of moderate heat flow (67 mW m^{-2}), and a shield area with very low heat flow (41 mW m^{-2}). In both cases, the total force (equal to the area under the differential stress profile, and shown in the right-hand frames) equals 3×10^{12} N m^{-1}, in accordance with the force-limited steady-state failure equilibrium model illustrated in Figure 1. See text for details of the parameters used to construct these figures.

A downward continuation method was used to determine temperature at depth. We have incorporated a very simple heat productivity model, in which the heat productivities of the upper crust, lower crust, and lithospheric mantle are constant (cf. Pollack and Chapman, 1977; Chapman and Furlong, 1992); we further assumed thermal conductivity to be a function of both temperature and depth (Schatz and Simmons, 1972; Chapman and Furlong, 1992). The temperatures computed in this way are in good agreement with estimates from xenolith thermobarometry in shield areas (Rudnick and Nyblade, 1999).

Because intraplate regions are generally characterized by strike-slip/reverse faulting stress states (i.e., $S_1 > S_2 \sim S_3 \sim S_v$; see Zoback, 1992), we have incorporated this in the modeling presented below. We assume pore pressures in the lower crust to be nearly lithostatic, following the arguments presented by Nur and Walder (1990). The permeability of the lower crust probably does not exceed 10^{-19} m^2 at 30 km depth (Manning and Ingebritsen, 1999), implying relatively long characteristic diffusion times (>10^5 years), and that nearly lithostatic pore pressures are likely to be maintained. The reason for this is that at elevated temperatures, a number of processes of permeability reduction (chemical precipitation, inelastic deformation, etc.) are expected to occur at rates sufficient to preclude rapid fluid migration, and hence to favor high pore pressures.

Given a temperature–depth profile, we can calculate differential stresses in the ductile portion of

the upper and lower crust and lithospheric mantle and the corresponding ductile strain rate, $\dot{\varepsilon}$ (Eq. 1), such that the cumulative area under the stress profile not exceed the assumed constraint of 3×10^{12} N m^{-1}. Figure 6 illustrates temperature and differential stress profiles for two end-member intraplate regions (which differ only in terms of their average surface heat flow) as well as the corresponding cumulative strength profiles and strain rates. In the upper part of the figure, we consider an area with moderately high heat flow (67 mW m^{-2}). Because of relatively high temperatures in the lower crust and upper mantle, relatively little force is required to cause deformation there. Thus, relatively high strain rates are achieved (~10^{-16} s^{-1}), and on geologic time scales the area would appear to deform as a viscous continuum. Note that in this case, most of the total tectonic force is carried in the strong brittle crust. In the lower half of Figure 6, we consider a cold shield area. In this case, the lower crust and upper mantle are considerably stronger and the total force available is sufficient to cause strain at a rate of only ~10^{-29} s^{-1}, a negligible rate (even over billions of years!) and thus consistent with a rigid plate assumption.

Because calculations such as those in Figure 6 involve a large number of parameters (surface heat flow, thermal conductivity, upper-crustal heat productivity, the frictional coefficient of the crust, and the rheological parameters of each layer), Zoback and Townend (2001) treated uncertainties in each of these parameters using a Monte Carlo technique: 1000 estimates of each parameter were drawn at random from normal distributions, and 1000 separate models were constructed. Composite temperature–depth, differential stress–depth, and strength–depth profiles were then constructed by stacking the different models' results.

Figure 7 illustrates the intraplate lithosphere modeling results for surface heat flow of 60 ± 6 mW m^{-2} (mean ± 10%), representative of stable continental heat flow (Pollack et al., 1993). The uppermost plots (a–c) display the model results incorporating hydrostatic pore pressures in the upper crust, and the three middle plots (d–f) display the corresponding results for near-lithostatic pore pressures. Note that the temperature–depth profiles are the same in both cases. At the bottom of the figure is a histogram (g) illustrating the range of estimated strain rates under each pore pressure condition: the strain rates are distributed log-normally about a geometric mean of approximately 10^{-18} s^{-1} under near-hydrostatic upper-crustal pore-pressure conditions, and approximately 10^{-15} s^{-1} for near-lithostatic pore pressure conditions. This latter value is much too high to be consistent with geologic and geodetic observations, and demonstrates the importance of near-hydrostatic fluid pressures in the upper crust for maintaining the strength of intraplate lithosphere. Although we do not illustrate it here, it is important to note that for very low surface heat flow (<50 ± 5 mW m^{-2}), such as is characteristic of Proterozoic and Archean cratonic crust (Pollack et al., 1993), strain rates lower than 10^{-20} s^{-1} are expected under either pore pressure regime.

Diffuse Deformation Along the San Andreas Fault System in Central California

In the previous section, we considered average intraplate deformation rates. Here we consider an example of how these arguments can be used to help interpret the broad zone of distributed transpressional deformation along the Pacific/North America plate boundary in western California.

As pointed out by Page et al. (1998), deformation along the San Andreas system is transpressional; in addition to the right-lateral shear accommodating relative motion between the Pacific and North American plates, appreciable convergence has been occurring since 3.5 Ma. This convergence has resulted in uplift, folding, and reverse faulting in the Coast Ranges, as illustrated by both the topographic relief (Fig. 8) and the currently active geologic structures, many of which accommodate shortening perpendicular to the San Andreas fault (Fig. 9, modified from Page et al., 1998). The locations of the two cross-sections in Figure 9 are indicated in Figure 8. Note that the transpressional deformation is accommodated over a broad region >100 km in width.

This type of distributed deformation might be categorized as a diffuse plate boundary (e.g., Gordon, 1998), but it is interesting to consider more specifically why the transpressional deformation is distributed so broadly, and why there is such an abrupt cessation of this deformation at the boundary between the Coast Ranges and the Great Valley (Figs. 8 and 9). The sharpness of this transition is particularly distinctive given that the entire region is subject to a relatively uniform compressive stress field acting at a high angle to the San Andreas fault and subparallel strike-slip faults (Fig. 8; Townend and Zoback, 2001). This high angle implies that the San Andreas fault (and perhaps other plate bound-

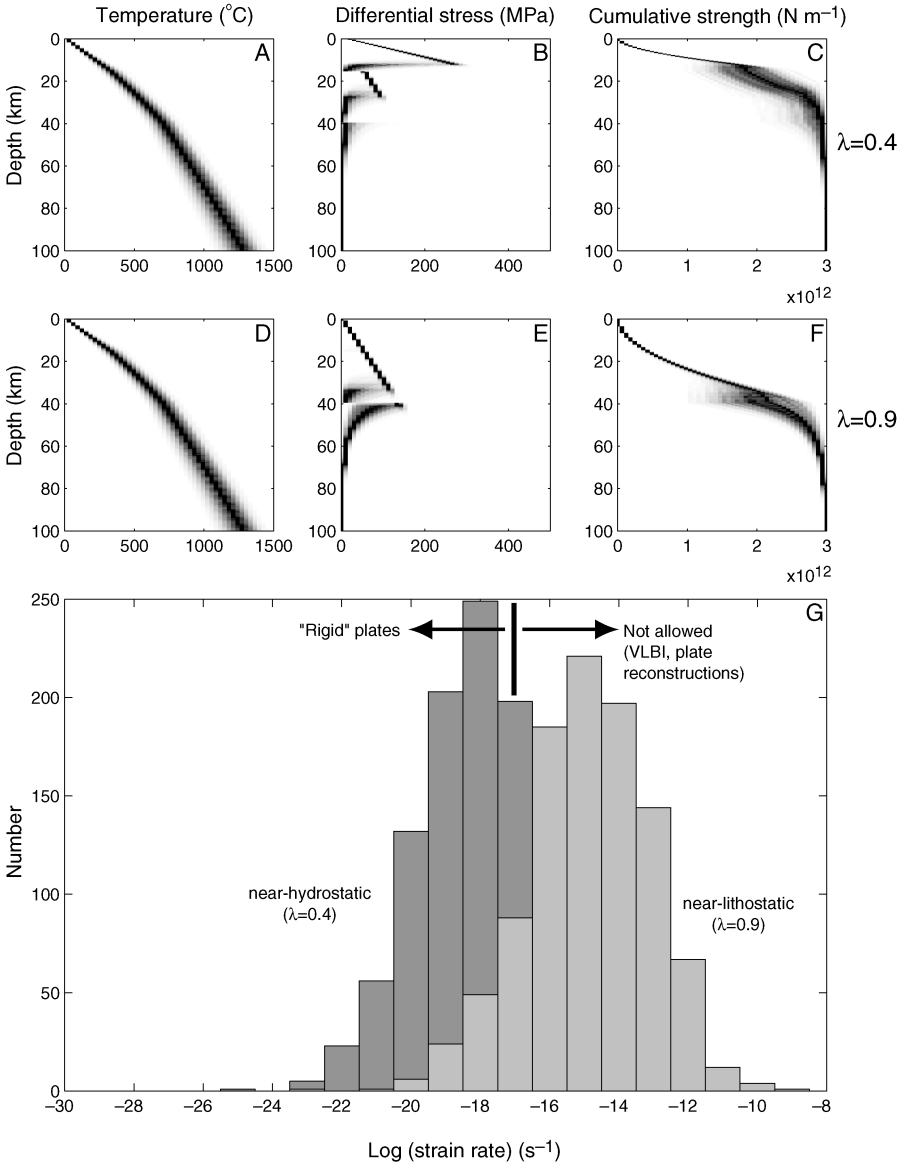

FIG. 7. Results of 1000 Monte Carlo strain-rate calculations for a strike-slip stress state and surface heat flow of 60 ± 6 mW m^{-2}, subject to the constraint that the total strength of the lithosphere is 3×10^{12} N m^{-1} (from Zoback and Townend, 2001). See text for explanation.

aries) have low frictional strength, in marked contrast to the high frictional strength exhibited by intraplate faults (briefly summarized by Zoback, 2000). Moreover, compressive deformation in the Coast Ranges ends abruptly at the Coast Range/Great Valley boundary, even though highly compressive stresses associated with reverse faulting are pervasive along the eastern edge of the Coast Ranges (Wentworth and Zoback, 1989).

It is also interesting to note that the stress observations shown in Figure 8 are remarkably consistent with modeled stress directions (dashed trajectories,

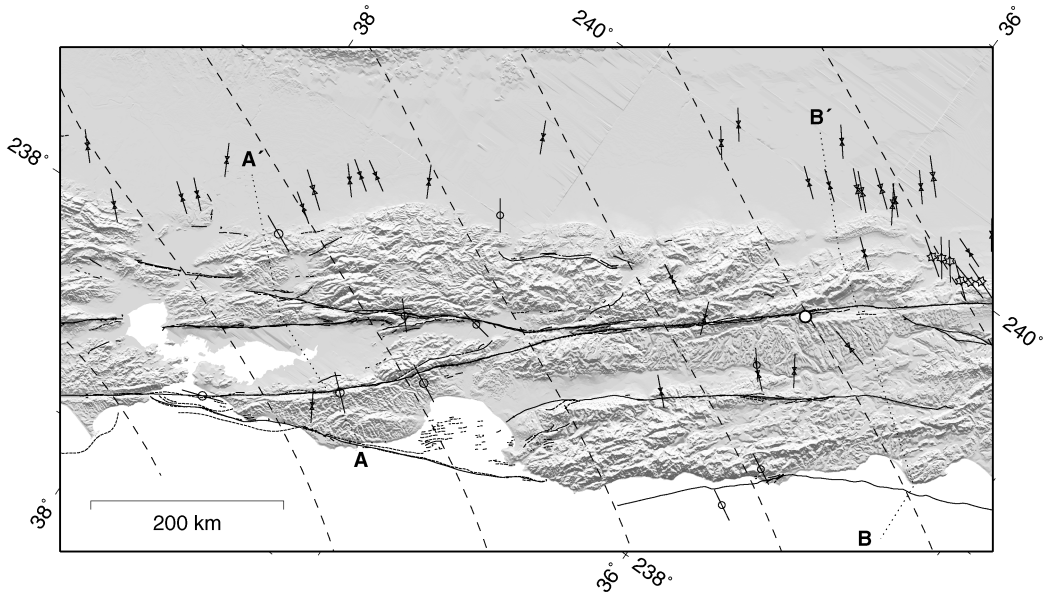

FIG. 8. Topographic map of western California in an oblique Mercator projection about the NUVEL 1A North America–Pacific Euler pole (DeMets et al., 1990). In this projection, relative plate motion is parallel to the upper and lower margins of the map. The major right-lateral strike-slip faults comprising the San Andreas fault system are also shown. The data show the direction of maximum horizontal stress from earthquake focal mechanism inversions (lines with a circle in the middle) or borehole stress measurements (bow-tie symbols). Most data are from theWorld Stress Map database [http://www-wsm.physik.uni-karlsruhe.de/index.html]. The dashed trajectories are interpolations of stress directions calculated by Flesch et al. (2000) using a model based on lithospheric buoyancy and plate interaction. Dotted lines A–A' and B–B' are lines of section shown in Figure 9.

interpolated from the results of Flesch et al., 2000). The Flesch et al. model incorporates the combined effects of buoyancy-related stresses in the western United States (principally due to the thermally uplifted Basin and Range province) and right-lateral shear in the far field associated with plate interaction. As discussed by Zoback et al. (1987), the stress data shown in Figure 8 were mainly obtained from stress-induced wellbore breakout measurements in oil and gas wells, and earthquake focal mechanisms that are not associated with right-lateral slip along transform faults.

To explain this abrupt change in the rate of deformation at the boundary between the Coast Ranges and the Great Valley in terms of the principles discussed above, it is important to note that the edge of the transpressive deformation coincides with a marked decrease in heat flow (Fig. 9), and therefore with a lateral variation in lithosperic temperatures. In other words, the rate of deformation is high throughout the Coast Ranges because temperatures in the lower crust and upper mantle are high. In contrast, heat flow in the Great Valley is extremely low (comparable to that of shield areas); hence the available force is insufficient to cause deformation at appreciable rates. In fact, as revealed by undeformed seismic reflectors corresponding to formations as old as Cretaceous in age, it is remarkable how little deformation has occurred in the Great Valley during the Cenozoic (e.g., Wentworth and Zoback, 1989).

Localized Deformation in Intraplate Seismic Areas

As is well known regarding eastern North America and Western Europe (Fig. 10), seismicity in intraplate regions is not homogeneously distributed, but is instead localized in areas of concentrated seismicity. While the instrumentally recorded seismicity illustrated in Figure 10 represents only a short period of time, it is clear that some intraplate

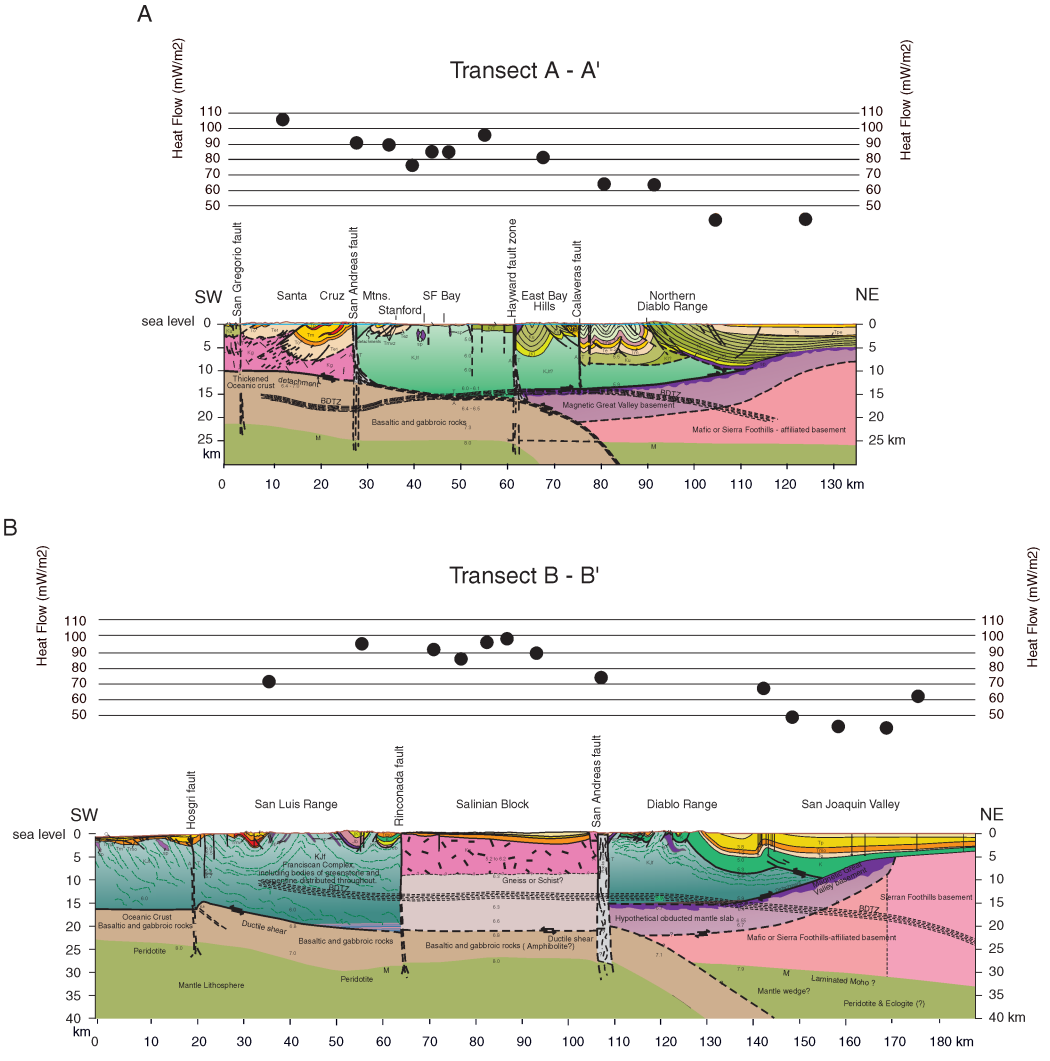

FIG. 9. Geologic cross-sections and heat-flow data across the Coast Ranges and San Andreas fault system in (A) Transect A–A' (shown in Fig. 8) through the Santa Cruz Mountains and the San Francisco Bay area and (B) Transect B–B' through central California near San Luis Obispo and Kettleman Hills (simplified from Page et al., 1998).

areas have been sites of pronounced and recurrent seismicity.

One example of a seismically active intraplate area undergoing localized deformation is the New Madrid seismic zone (NMSZ, Fig. 11), which experienced three major earthquakes in 1811–1812. Paleo-liquefaction data suggest that very large, 1811–1812 type events have occurred every 200–900 years during the past several thousand years (Tuttle and Schweig, 1995; Tuttle et al., 1999). These prehistoric events, along with the 1811–1812 earthquakes themselves, must have had moment magnitudes of 7.5, or greater, to have caused the severe liquefaction observed over large parts of the New Madrid region. However, extensive seismic reflection data in the NMSZ reveal relatively small cumulative fault offsets in the post-Cretaceous Mississippi embayment sediments (e.g., Hamilton and Zoback, 1981), implying that the level of seismicity observed in late Holocene time must have begun relatively recently (Schweig and Ellis, 1994).

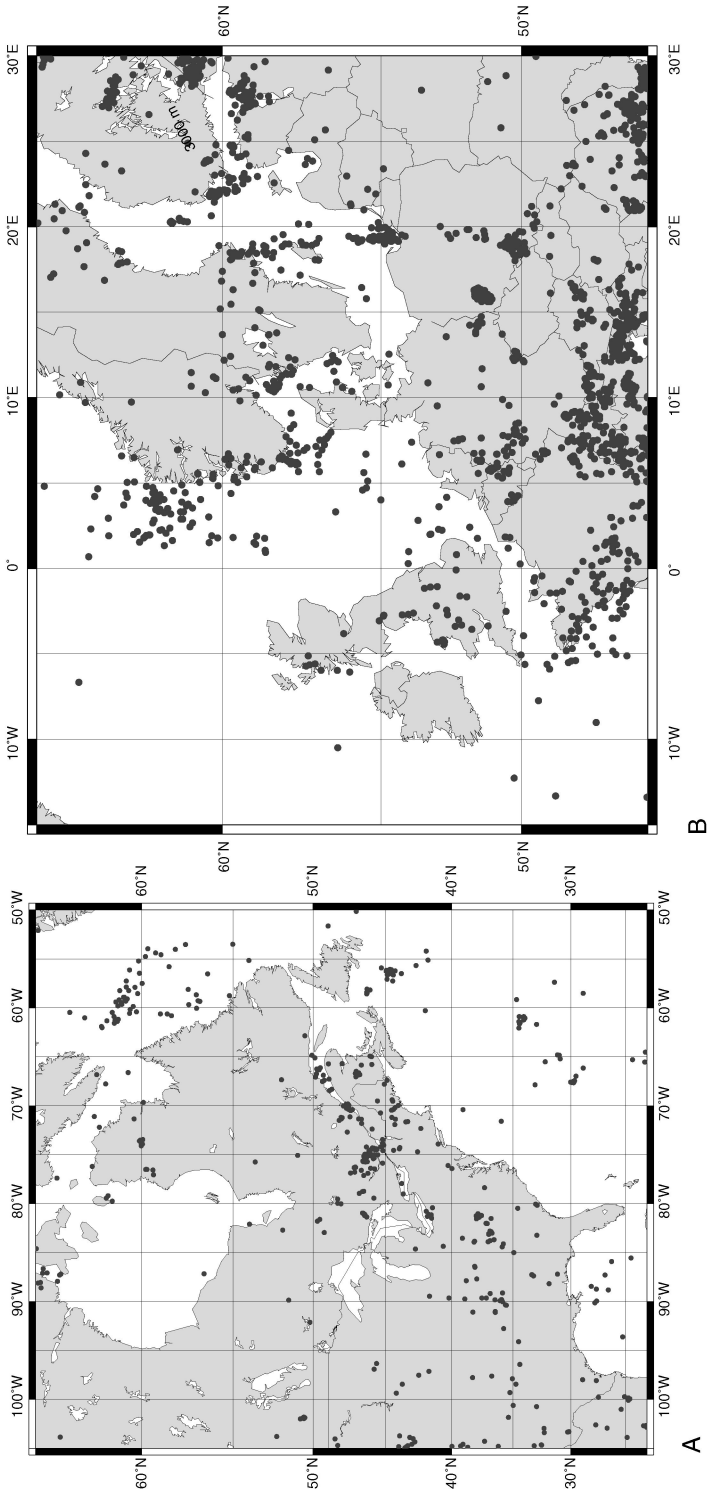

FIG. 10. Instrumentally recorded seismicity in eastern North America (left) and western Europe (right), illustrating the heterogeneous distribution of seismicity.

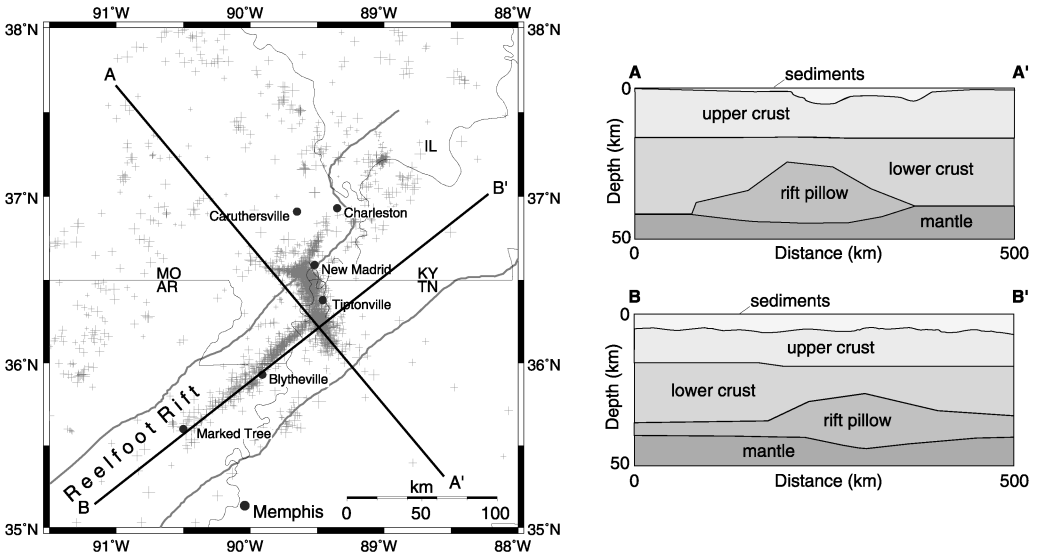

FIG. 11. A map of the New Madrid seismic zone and crustal structure based on gravity and seismic data along two profiles parallel and perpendicular to the Reelfoot rift (from Grollimund and Zoback, 2001, with original data from Mooney et al., 1983 and Stuart et al., 1997).

The NMSZ is broadly associated with an ancient intraplate rift zone that was active principally during the latest Precambrian or Early Paleozoic (e.g., McKeown, 1982). Geological and geophysical data also indicate an episode of Cretaceous alkaline magmatic activity (Zoback et al., 1980; Hildenbrand, 1985). As a result, the crustal structure in the NMSZ is quite anomalous with respect to the surrounding region.

Several hypotheses have been proposed to account for the mechanical role of this anomalous crustal structure in localizing seismicity within the NMSZ. One suggestion is the existence of a local stress concentration caused by either a rift pillow (Grana and Richardson, 1996) or an associated subhorizontal detachment fault (Stuart et al., 1997). Liu and Zoback (1997) suggested that the high rate of seismicity is a result of elevated heat flow causing high ductile strain rates in the lower crust and upper mantle. Unfortunately, none of these hypotheses satisfactorily explains the apparently sudden onset of seismicity during the Holocene.

Grollimund and Zoback (2001) investigated the interaction between anomalous crustal structure and stress changes caused by deglaciation, based on the striking temporal coincidence between melting of the Laurentide ice sheet (~19–8 ka, Fig. 12), and

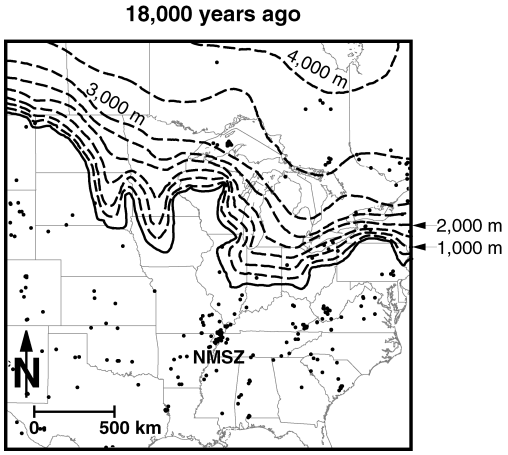

FIG. 12. Distribution of M > 3.5 earthquakes in eastern North America and the maximum extent and thickness of the Laurentide ice sheet at approximately 20 ka.

the occurrence of increased seismicity in the Late Holocene. Stein et al. (1979, 1989) had previously discussed deglaciation as a perturbing mechanism capable of inducing earthquakes in intraplate areas, specifically along passive margins such as north-

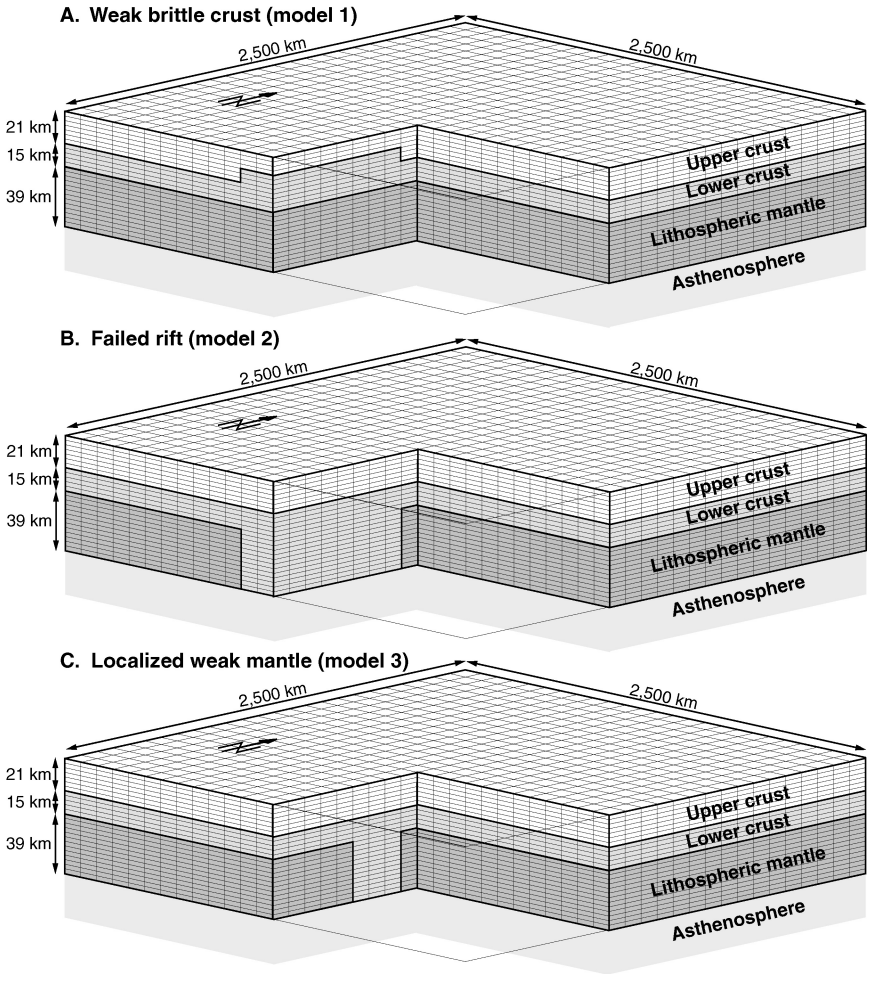

FIG. 13. The three models of anomalous crust and upper mantle structure in the New Madrid seismic zone considered by Grollimund and Zoback (2001).

eastern North America. Using a highly simplified ice-sheet geometry and lithospheric structure, James and Bent (1994) demonstrated that deglaciation could significantly affect crustal strain rates at distances of several hundred kilometers from the ice front. They concluded, however, that deglaciation did not promote seismicity in the New Madrid area. Wu and Johnston (2000) used a more realistic ice-sheet geometry and concluded that deglaciation could have triggered seismicity in the general New Madrid area. However, their model predicted that the onset of seismicity was only 200 years ago, and the region of predicted seismicity was not confined to the NMSZ.

Grollimund and Zoback (2001) used three-dimensional finite element models (Fig. 13) to explore the coupled interaction between plate driving forces, stress perturbations caused by deglaciation, and heterogeneous lithospheric properties. They adopted relatively simple geometric representations of the mantle, and focused primarily on anomalous lower-crust and upper-mantle structure associated with the ancient rift (Fig. 13). They showed that the lithospheric response to removal of the Laurentide ice sheet (starting at ~20 ka), changed the stress field in the vicinity of New Madrid in such a way as to increase seismic strain rates by about three orders of magnitude (Fig. 14).

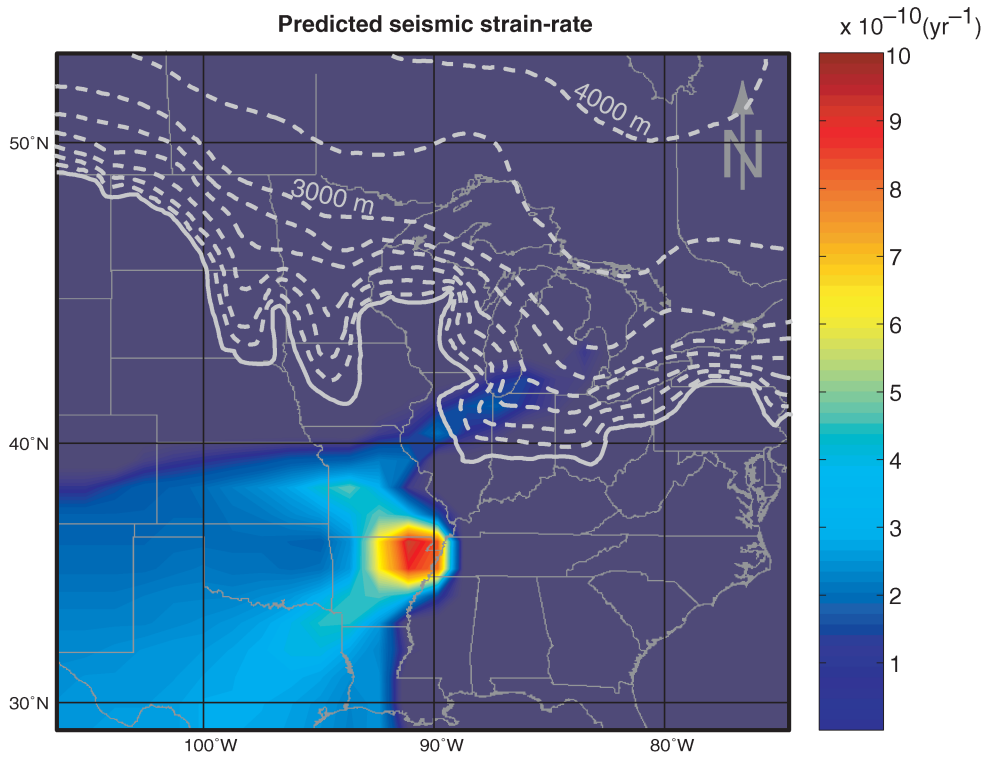

FIG. 14. Concentration of high predicted strain rates in the New Madrid seismic zone resulting from deglaciation-induced lithospheric flexure (from Grollimund and Zoback, 2001). The strain rate is approximately three orders of magnitude higher than in the surrounding regions.

With respect to seismic hazards in the region, it is important to note that Grollimund and Zoback's modeling predicts that the high rate of seismic energy release observed during Late Holocene time is likely to remain approximately constant for the next few thousand years.

The spatial confinement of seismicity appears to be a direct result of anomalous lithospheric properties associated with the ancient Precambrian rift. The best-fitting model involves a one-order-of-magnitude decrease in upper-mantle viscosity beneath the NMSZ with respect to the mantle elsewhere. This seems plausible for two reasons: depletion of the upper mantle beneath a rift zone is to be expected as a consequence of the formation of an anomalously dense lower-crustal "pillow" (Fig. 11). In addition, the occurrence of post-Late Cretaceous or Early Tertiary volcanism may imply the existence of anomalous, low-viscosity upper mantle.

Conclusions

Numerous data obtained from deep boreholes worldwide reveal that upper-crustal permeabilities are sufficiently high (10^{-17} to 10^{-16} m^2) for pore pressures to attain hydrostatic values over geologically short periods of time (less than ~1000 years). These high permeabilities appear to be maintained by hydraulically conductive, critically stressed faults, which also limit the strength of the brittle crust. As the ductile lithosphere is expected to creep in response to any finite differential stress (based on the form of laboratory-derived constitutive laws), the rate of lithospheric deformation is con-

trolled both by the strength of the ductile lower crust and upper mantle (and therefore by temperature and composition), and by the magnitude of the applied tectonic force. In terms of this simple model, crustal stress is expected to be high, even in relatively stable Phanerozoic intraplate regions, as well as in Archean and Proterozoic shields. This has been verified, for example, by stress data obtained from deep boreholes drilled in southeastern Germany and Sweden.

We have used a total-force constraint on models of lithospheric strength profiles to determine the strain rates at which intraplate lithosphere deforms, given the observed high frictional strength and generally hydrostatic upper-crustal pore pressures. We estimate that the strike-slip stress regimes and thermal conditions characteristic of stable continental regions, are associated with strain rates less than 10^{-17} s^{-1}. The lithosphere cannot deform more rapidly than this because of the limited amount of tectonic force available to drive deformation.

In the context of the steady-state failure equilibrium model, the debate over whether intraplate deformation is best viewed in terms of a deforming continuum or rigid crustal blocks separated by relatively weak fault zones may be a false dichotomy because both types of behavior are to be expected. As illustrated for the Coast Ranges and Central Valley of western California, in the area of presumed high temperatures in the lower crust and upper mantle (the Coast Ranges), the strong temperature dependence of the effective viscosity of the lower crust and upper mantle results in high deformation rates. In the adjacent Central Valley, where we expect low temperatures in the lower crust and upper mantle, the lithospere is observed, as anticipated, to deform at an extremely slow rate.

The Holocene concentration of intraplate seismicity in the New Madrid seismic zone appears to result from three principal factors. First, the lithosphere is in a state of failure equilibrium such that relatively small stress perturbations can produce significant changes in deformation rates. Second, anomalous upper-mantle structure beneath the New Madrid region plausibly exists as a result of geologic processes that have occurred recurrently since as early as the Late Precambrian or Early Paleozoic. Finally, the stress perturbation caused by deglaciation, while small in comparison to the total strength of the lithosphere, appears to have been sufficient to cause substantial ductile strain in the upper mantle, and a correspondingly high rate of brittle failure in the upper crust. The first factor, the critically stressed brittle crust, allows a relatively small stress perturbation to trigger brittle faulting, and viscous flow in the lower crust and upper mantle to cause multiple earthquakes through time. The second factor, an anomalous upper mantle structure in the area of the rift, serves to localize seismicity in the New Madrid region. The third factor, the perturbation associated with deglaciation, is responsible for the concentration of activity in Holocene time. It is interesting to speculate whether similar factors might also be responsible for the apparent concentrations of seismicity in other intraplate seismic areas in the world.

Acknowledgments

This paper was presented at a symposium honoring the career and contributions of George A. Thompson held on December 8 and 9, 2001 at Stanford University. It is a pleasure to acknowledge George's advice and assistance to us as a colleague, teacher, and mentor. We thank Norm Sleep and Björn Lund, and the editors, Gary Ernst and Simon Klemperer, for their thoughtful reviews.

REFERENCES

Anderson, J. G., 1986, Seismic strain rates in the central and eastern United States: Bulletin of the Seismological Society of America, v. 76, p. 273–290.

Barton, C. A., Hickman, S. H., Morin, R., Zoback, M. D., and Benoit, D., 1998, Reservoir-scale fracture permeability in the Dixie Valley, Nevada, geothermal field: Abstracts Volume, Society of Petroleum Engineers Annual Meeting, Trondheim, Norway, Paper Number 47371, p. 315–322.

Barton, C. A., Zoback, M. D., and Moos, D., 1995, Fluid flow along potentially active faults in crystalline rock: Geology, v. 23, p. 683–686.

Bott, M. H. P., and Kusznir, N. J., 1984, The origin of tectonic stress in the lithosphere: Tectonophysics, v. 105, p. 1–13.

Brace, W. F., and Kohlstedt, D. L., 1980, Limits on lithospheric stress imposed by laboratory experiments: Journal of Geophysical Research, v. 85, p. 6248–6252.

Brudy, M., Zoback, M. D., Fuchs, K., Rummel, F., and Baumgärtner, J., 1997, Estimation of the complete stress tensor to 8 km depth in the KTB scientific drill holes: Implications for crustal strength: Journal of Geophysical Research, v. 102, p. 18,453–18,475.

Byerlee, J. D., 1978, Friction of rocks: Pure and Applied Geophysics, v. 116, p. 615–626.

Carter, N. L., and Tsenn, M. C., 1987, Flow properties of continental lithosphere: Tectonophysics, v. 136, p. 27–63.

Chapman, D. S., and Furlong, K. P., 1992, Thermal state of the continental lower crust, *in* Fountain, D. M., Arculus, R., and Kay, R. W., eds., Continental lower crust: Amsterdam, Netherlands, Elsevier Science Publishers, p. 179–199.

Chen, W.-P., and Molnar, P., 1983, Focal depths of intracontinental and intraplate earthquakes and their implications for the thermal and mechanical properties of the lithosphere: Journal of Geophysical Research, v. 88, p. 4183–4214.

Chopra, P. N., and Paterson, M. S., 1981, The experimental deformation of dunite: Tectonophysics, v. 78, p. 453–473.

Christensen, N. I., and Mooney, W. D., 1995, Seismic velocity structure and composition of the continental crust: A global view: Journal of Geophysical Research, v. 100, p. 9761–9788.

DeMets, C., Gordon, R. G., Argus, D. F., and Stein, S., 1990, Current plate motions: Geophysical Journal International, v. 101, p. 425–478.

England, P. C., and Houseman, G. A., 1986, Finite strain calculations of continental deformation, 2, comparison with the India–Asia collision zone: Journal of Geophysical Research, v. 91, p. 3664–3676.

Flesch, L. M., Haines, A. J., and Holt, W. E., 2001, Dynamics of the India-Eurasia collision zone: Journal of Geophysical Research, v. 106, p. 16,435–16,460.

Flesch, L. M., Holt, W. E., Haines, A. J., and Shen-Tu, B., 2000, Dynamics of the Pacific–North American plate boundary in the western United States: Science, v. 287, p. 834–836.

Forsyth, D., and Uyeda, S., 1975, On the relative importance of the driving forces of plate motion: Geophysical Journal of the Royal Astronomical Society, v. 43, p. 163–200.

Gordon, R. G., 1998, The plate tectonic approximation: Plate non-rigidity, diffuse plate boundaries, and global plate reconstructions: Annual Review of Earth and Planetary Sciences, v. 26, p. 615–642.

Grana, J. P., and Richardson, R., 1996, Tectonic stress within the New Madrid seismic zone: Journal of Geophysical Research, v. 101, p. 5445–5458.

Grollimund, B., and Zoback, M.D., 2001, Did deglaciation trigger New Madrid seismicity?: Geology, v. 29, p. 175–178.

Hamilton, R. M., and Zoback, M. D., 1981, Tectonic features of the New Madrid seismic zone from seismic reflection profiles: U.S. Geological Survey Professional Paper, 1236-F, p. 55–82.

Healy, J. H., Rubey, W. W., Griggs, D. T., and Raleigh, C. B., 1968, The Denver earthquakes: Science, v. 161, p. 1301–1310.

Hickman, S. H., Barton, C. A., Zoback, M. D., Morin, R., Sass, J., and Benoit, R., 1997, In situ stress and fracture permeability along the Stillwater fault zone, Dixie Valley, Nevada: International Journal of Rock Mechanics and Mining Sciences, v. 34, Paper No. 126, p. 414.

Hildenbrand, T. G., 1985, Rift structure of the northern Mississippi Embayment from the analysis of gravity and magnetic data: Journal of Geophysical Research, v. 90, p. 12,607–12,622.

Hubbert, M. K., and Rubey, W. W., 1959, Role of fluid pressure in the mechanics of overthrust faulting: Geological Society of America Bulletin, v. 70, p. 115–205.

Ito, T., and Zoback, M. D., 2000, Fracture permeability and in situ stress to 7 km depth in the KTB scientific drillhole: Geophysical Research Letters, v. 27, p. 1045–1048.

Jaeger, J. C., and Cook, N. G. W., 1979, Fundamentals of rock mechanics: London, UK, Chapman and Hall, 593 p.

James, T. S., and Bent, A. L., 1994, A comparison of eastern North American seismic strain-rates to glacial rebound strain-rates: Geophysical Research Letters, v. 21, p. 2127–2130.

Jones, C. H., Unruh, J.R., and Sonder, L. J., 1996, The role of gravitational potential energy in active deformation in the southwestern United States: Nature, v. 381, 37–41.

Kohlstedt, D. L., Evans, B., and Mackwell, S. J., 1995, Strength of the lithosphere: Constraints imposed by laboratory experiments: Journal of Geophysical Research, v. 100, p. 17,587–17,602.

Kusznir, N. J., 1991, The distribution of stress with depth in the lithosphere: Thermo-rheological and geodynamic constraints, *in* Whitmarsh, R. B., ed., Tectonic stress in the lithosphere: London, UK, The Royal Society, p. 95–107.

Liu, L., and Zoback, M. D., 1997, Lithospheric strength and intraplate seismicity in the New Madrid seismic zone: Tectonics, v. 16, p. 585–595.

Lund, B., and Zoback, M. D., 1999, Orientation and magnitude of in situ stress to 6.5 km depth in the Baltic Shield: International Journal of Rock Mechanics and Mining Sciences, v. 36, p. 169–190.

Manning, C. E., and Ingebritsen, S. E., 1999, Permeability of the continental crust: Implications of geothermal data and metamorphic systems: Reviews of Geophysics, v. 37, p. 127–150.

McGarr, A., and Gay, N. C., 1978, State of stress in the Earth's crust: Annual Review of Earth and Planetary Sciences, v. 6, p. 405–436.

McKeown, F., 1982, Overview and discussion: U.S. Geological Survey Professional Paper, v. 1236, p. 1–14.

Mooney, W. D., Andrews, M. C., Ginzburg, A., Peters, D. A., and Hamilton, R. M., 1983, Crustal structure of the northern Mississippi Embayment and a comparison with other continental rift zones: Tectonophysics, v. 94, p. 327–348.

Nur, A., and Walder, J., 1990, Time-dependent hydraulics of the earth's crust, *in* Bredehoeft, J. D., and Norton,

D. L., eds., The role of fluids in crustal processes: Washington, DC, National Academy Press, p. 113–127.

Page, B. M., Thompson, G. A., and Coleman, R. G., 1998, Late Cenozoic tectonics of the central and southern Coast Ranges of California: Geological Society of America Bulletin, v. 110, p. 846–876.

Pine, R. J., Ledingham, P., and Merrifield, C. M., 1983, In situ stress measurements in the Carnmenellis granite—II. Hydrofracture tests at Rosemanowes Quarry to depths of 2000 m: International Journal of Rock Mechanics and Mining Sciences/Geomechanics Abstracts, v. 20, p. 63–72.

Pollack, H. N., and Chapman, D. S., 1977, On the regional variation of heat flow, geotherms and lithosphere thickness: Tectonophysics, v. 38, p. 279–396.

Pollack, H. N., Hurter, S. J., and Johnson, J. R., 1993, Heat flow from the Earth's interior; analysis of the global data set: Reviews of Geophysics, v. 31, p. 267–280.

Ranalli, G., and Murphy, D. C., 1987, Rheological stratification of the lithosphere: Tectonophysics, v. 132, p. 281–295.

Roeloffs, E., 1996, Poroelastic techniques in the study of earthquake-related hydrologic phenomena: Advances in Geophysics, v. 37, p. 135–195.

Rudnick, R. L., and Nyblade, A. A., 1999, The thickness and heat production of Archean lithosphere: Constraints from xenolith thermobarometry and surface heat flow, *in* Fei, Y., Bertka, C., and Mysen, B., eds., Mantle petrology: Field observations and high pressure experimentation: The Geochemical Society, Special Publication, no. 6, p. 3–12.

Schatz, J. P., and Simmons, G., 1972, Thermal conductivity of earth materials at high temperatures: Journal of Geophysical Research, v. 77, p. 6922–2983.

Schweig, E. S., and Ellis, M. A., 1994, Reconciling short recurrence intervals with minor deformation in the New Madrid seismic zone: Science, v. 264, p. 1308–1311.

Sibson, R. H., 1974, Frictional constraints on thrust, wrench, and normal faults: Nature, v. 249, p. 542–544.

_____, 1983, Continental fault structure and the shallow earthquake source: Journal of the Geological Society of London, v. 140, p. 741–767.

Simpson, D. W., Leith, W. S., and Scholz, C. H., 1988, Two types of reservoir-induced seismicity: Bulletin of the Seismological Society of America, v. 78, p. 2025–2040.

Stein, R. S., Barka, A. A., and Dieterich, J. H., 1997, Progressive failure on the North Anatolian fault since 1939 by earthquake stress triggering: Geophysical Journal International, v. 128, p. 594–604.

Stein, R. S., King, G. C., and Lin, J., 1992, Change in failure stress on the southern San Andreas fault system caused by the 1992 magnitude = 7.4 Landers earthquake: Science, v. 258, p. 1328–1332.

Stein, S., Cloetingh, S., Sleep, N. H., and Wortel, R., 1989, Passive margin earthquakes, stresses, and rheology: Earthquakes at North Atlantic passive margins, *in* Gregersen, S., and Basham, P. W., eds., Neotectonics and postglacial rebound: Dordrecht, Netherlands, Kluwer, p. 231–259.

Stein, S., Sleep, N., Geller, R., Wang, S., and Kroeger, G., 1979, Earthquakes along the passive margin of eastern Canada: Geophysical Research Letters, v. 6, p. 537–540.

Stuart, W. D., Hildenbrand, T. G., and Simpson, R. W., 1997, Stressing of the New Madrid Seismic Zone by a lower crust detachment fault: Journal of Geophysical Research, v. 102, p. 27,623–27,633.

Townend, J., and Zoback, M. D., 2000, How faulting keeps the crust strong, Geology, v. 28, p. 399–402.

_____, 2001, Implications of earthquake focal mechanisms for the frictional strength of the San Andreas fault system, *in* Holdsworth, R. E., Strachan, R. A., Magloughlin, J. F., and Knipe, R. J., eds., The nature and tectonic significance of fault zone weakening: Geological Society of London, Special Publications, v. 106, p. 13–21.

Turcotte, D. L., and Schubert, G., 1982, Geodynamics: New York, NY, John Wiley & Sons, 450 p.

Tuttle, M., Chester, J., Lafferty, R., Dyer-Williams, K., and Cande, R., 1999, Paleoseismology study northwest of the New Madrid Seismic Zone: Washington, DC, Report prepared for U.S. Nuclear Regulatory Commission, Division of Engineering Technology, 96 p.

Tuttle, M. P., and Schweig, E. S., 1995, Archeological and pedological evidence for large prehistoric earthquakes in the New Madrid seismic zone, central United States: Geology, v. 23, p. 253–256.

Wentworth, C. M., and Zoback, M. D., 1989, The style of late Cenozoic deformation at the eastern front of the California Coast Ranges: Tectonics, v. 8, p. 237–246.

Wilks, K. R., and Carter, N. L., 1990, Rheology of some continental lower crustal rocks: Tectonophysics, v. 182, p. 57–77.

Wu, P., and Johnston, P., 2000, Can deglaciation trigger earthquakes in North America?: Geophysical Research Letters, v. 27, p. 1323–1326.

Zoback, M. D., 2000, Strength of the San Andreas: Nature, v. 405, p. 31–32.

Zoback, M. D., Hamilton, R. M., Crone, A. J., Russ, D. P., McKeown, F. A., and Brockman, S. R., 1980, Recurrent intraplate tectonism in the New Madrid seismic zone: Science, v. 209, p. 971–976.

Zoback, M. D., and Harjes, H.-P., 1997, Injection-induced earthquakes and crustal stress at 9 km depth at the KTB deep drilling site, Germany: Journal of Geophysical Research, v. 102, p. 18,477–18,491.

Zoback, M. D., and Healy, J. H., 1992, In situ stress measurements to 3.5 km depth in the Cajon Pass scientific research borehole: Implications for the mechanics of crustal faulting: Journal of Geophysical Research, v. 97, p. 5039–5057.

Zoback, M. D., et al., 1987, New evidence on the state of stress of the San Andreas fault system: Science, v. 238, p. 1105–1111.

Zoback, M. D., and Townend, J., 2001, Implications of hydrostatic pore pressures and high crustal strength for the deformation of intraplate lithosphere: Tectonophysics, v. 336, p. 19–30.

Zoback, M. D., and Zoback, M. L., 1991, Tectonic stress field of North America and relative plate motions, *in* Slemmons, D. L., Engdahl, E. R., Zoback, M. D., and Blackwell, M. D., eds., Neotectonics of North America: Boulder, Colorado, Geological Society of America, p. 339–366.

Zoback, M. L., 1992, First- and second-order patterns of stress in the lithosphere: The World Stress Map project: Journal of Geophysical Research, v. 97, p. 11,703–11,728.

Zoback, M. L., and Zoback, M. D., 1980, State of stress in the conterminous United States: Journal of Geophysical Research, v. 85, p. 6113–6156.

_____, 1989, Tectonic stress field of the continental United States, *in* Pakiser, L. C., and Mooney, W. D., eds., Geophysical framework of the continental United States: Geological Society of America, v. 172, p. 523–539.